

All-Polymer Solar Cells from Perylene Diimide Based Copolymers: Material Design and Phase Separation Control

Erjun Zhou, Junzi Cong, Qingshuo Wei, Keisuke Tajima,* Chunhe Yang, and Kazuhito Hashimoto*

In recent years, polymer solar cells (PSCs) have received much attention because of their unique advantages such as low cost, light weight, ease of fabrication by large-scale, roll-to-roll printing techniques, and feasibility of flexible devices.^[1] To date, mixed bulk heterojunction (BHJ) PSCs based on interpenetrating networks of semiconducting polymers and fullerene derivatives have shown the best performance with state-of-the-art power-conversion efficiencies (PCEs) that exceed 7%.^[2]

All-polymer solar cells (all-PSCs), in which an n-type semiconducting polymer is used as the electron acceptor instead of a fullerene derivative have some unique advantages over polymer/fullerene BHJs for the following reasons. Firstly and most importantly, semiconducting polymers have high absorption coefficients in the spectral region of visible light, while fullerene derivatives only absorb photons within a very limited range of the solar spectrum. Although C₇₀ derivatives provide enhanced absorption in the blue region compared to C₆₀ derivatives,^[3] it is quite difficult to extend the response of fullerene derivatives into the red and near-infrared regions. Secondly, n-type polymers have a large potential for fine-tuning of energy levels, owing to their structural variety, which is crucial for the achievement of high performances in PSCs. A low-lying lowest unoccupied molecular orbital (LUMO) of the acceptor can result in more efficient photoinduced charge separation at donor/acceptor interfaces, but an excessively low LUMO will reduce the open-circuit voltage (V_{OC}) of PSCs.^[4] As a result, careful adjustment of the energy levels is required to maximize the total efficiency. Although a few examples of the fullerene derivatives have shown that tuning of the energy levels results in improved performance,^[5] chemical derivatives of fullerene structures are limited. In addition, polymer/polymer blends offer superior flexibility in controlling solution viscosity, an important factor in large-scale solution processes for film coating.

Because of the above-mentioned advantages of all-PSCs, much research has been performed on this kind of solar cells to search for effective combinations of donor/acceptor polymers by tailoring both components individually to optimize the optical properties, energy levels, charge transport, as well as charge-collection processes in an operating device.^[6] The main obstacle in all-PSC research is the limited number of effective n-type polymers. One strategy for the design of n-type polymers is to introduce strong electron-withdrawing groups into the polymer backbone. Cyano(CN)- and 2,1,3-benzothiadiazole(BT)-based n-type polymers are the most important and successful systems and PCE of all-PSCs reached 2% by extensive device optimization.^[7]

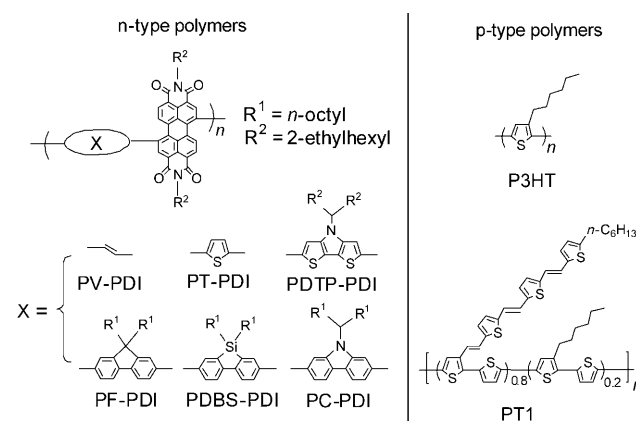
Perylene diimide(PDI)-based polymers have recently emerged as a new class of n-type polymers for application in PSCs. A PDI-based polymer was first used in all-PSCs in 2007 by Zhan et al.^[8] After optimization in terms of both material and device structure, a PCE of 1.46% as the highest value was obtained under the irradiation of AM 1.5 simulated solar light (100 mW cm⁻²).^[9] As an electron-deficient (acceptor) segment, PDI can be copolymerized easily with a wide variety of electron-rich (donor) units to tailor the optoelectronic properties of the resulting polymers.

In this study, we synthesized six PDI-based polymers (PX-PDIs) by combination of PDIs with different donor segments (X), including vinylene (V), thiophene (T), dithieno[3,2-*b*:2',3'-*d*]pyrrole (DTP), fluorene (F), dibenzosilole (DBS), and carbazole (C, see Scheme 1) and utilized them as n-type polymers for all-PSC applications. By gradually changing the electron-donating ability of the X parts, we attempted to fine-tune the physical properties of PDI-based polymers suitable for all-PSC applications.

[*] Dr. K. Tajima, Prof. K. Hashimoto
 Department of Applied Chemistry, School of Engineering
 The University of Tokyo
 7-3-1 Hongo, Bunkyo-ku, Tokyo 113-8656 (Japan)
 E-mail: k-tajima@light.t.u-tokyo.ac.jp
 hashimoto@light.t.u-tokyo.ac.jp

Dr. E. J. Zhou, J. Z. Cong, Dr. Q. S. Wei, Dr. K. Tajima, Dr. C. H. Yang,
 Prof. K. Hashimoto
 HASHIMOTO Light Energy Conversion Project
 Exploratory Research for Advanced Technology (ERATO, Japan)
 Science Technology Agency (JST, Japan)

Supporting information for this article is available on the WWW under <http://dx.doi.org/10.1002/anie.201005408>.



Scheme 1. Structures of six n-type PDI-based polymers and two p-type polythiophene derivatives.

On the other hand, the choice of the p-type polymers combined with the acceptor is also crucial for all-PSCs. Among the wide variety of p-type photovoltaic polymers, regioregular P3HT has been extensively studied by blending it with fullerene derivatives^[5] or n-type polymers.^[7] However, for combination with n-type polymers, P3HT might not necessarily be the best choice. Li et al. developed a series of conjugated side chain polythiophenes and applied them in both polymer/fullerene and all-polymer devices.^[10]

Herein, we used P3HT and a polythiophene derivative with conjugated side chains (PT1) as p-type semiconducting polymers (Scheme 1). We systematically investigated the photovoltaic properties by using all donor/acceptor combinations and analyzed the results from the viewpoints of the absorption spectra, the alignment of the energy levels, and the mixed morphology of the films.

The synthesis of six PX-PDIs is shown in Figure S1 in the Supporting Information. PV-PDI, PT-PDI, and PDTP-PDI were synthesized by the Stille coupling reaction and PF-PDI, PDBS-PDI, and PC-PDI were synthesized by the Suzuki coupling reaction as previously reported.^[9] For the donor material, P3HT was purchased from Merck Chemicals; PT1 was synthesized by the Stille reaction (Figure S2). All polymers show good solubility in common organic solvents, such as chloroform (CF), chlorobenzene (CB), *o*-dichlorobenzene (DCB), toluene, and xylene.

As mentioned earlier, the modulation of the absorption spectra of PDI-based polymers is crucial for the application of these polymers in all-PSCs. The absorption spectra of six PX-PDIs in film are shown in Figure 1. PV-PDI, PT-PDI, and

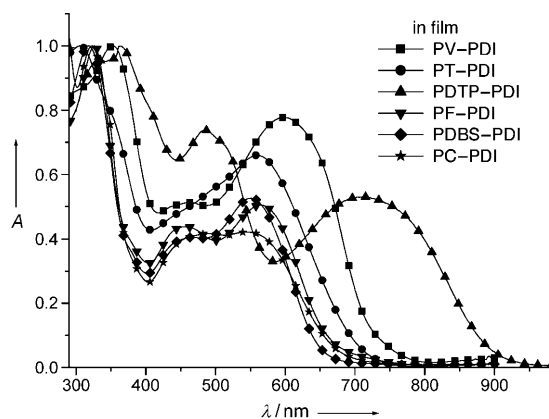


Figure 1. UV/Vis absorption spectra of six PX-PDI films on quartz plates.

PDTP-PDI show absorption in the relatively long-wavelength region probably because of the strong electron-donating ability of these donor units used, especially for PDTP-PDI, and/or the small steric hindrance of vinylene for PV-PDI. However, PDBS-PDI, PF-PDI, and PC-PDI absorb at relatively short wavelengths, which is attributable to the relatively weak electron-donating ability and large steric hindrance of bulky side chains in these donor building blocks, thus disturbing the planarity of the backbones. The absorption onsets of the six polymers in film also show a wide

range from 680 nm for PDBS-PDI to 940 nm for PDTP-PDI, thus proving that the absorption spectra could be tuned over a wide range by using donor segments with different electron-donating abilities. All these polymers show similar absorption spectra in CHCl_3 (Figure S3); the tuning over a wide range is highly useful for designing n-type polymers to complement the absorption of p-type polymers for all-PSC application.

The absorption spectra of PT1 and P3HT, both in chlorobenzene and in film, are shown in Figure S4. In solution, PT1 shows an absorption maximum at 476 nm, which is 20 nm red-shifted compared to that of P3HT, because of the enhanced conjugation caused by the tris(thienylenevinylene) side chain. In film, P3HT shows a large red-shift with an absorption maximum at 553 nm and a shoulder at approximately 600 nm, which corresponds to strong π - π stacking. In film, PT1, however, only shows a relatively small red-shift (21 nm), without any shoulder, probably because of its regiorandom structure. Although PT1 shows no improvement in its absorption spectra compared with P3HT, the introduction of a conjugated side chain may contribute to the charge transport to the corresponding electrodes.^[10]

The electrochemical properties of the six n-type polymers and two p-type polymers are also investigated by cyclic voltammetry (CV, Figure S5 and S6). All PDI-based polymers undergo reversible reductive n-doping/dedoping (reduction/reoxidation) processes, while only PDTP-PDI showed reversible p-doping/dedoping (oxidation/rereduction) processes. The reason for this behavior is not yet clear; however, it is speculated to be due to the high oxidation potential of the other five polymers. The highest occupied molecular orbital (HOMO) and LUMO energy levels of the conjugated polymers are calculated from the onset oxidation potential and onset reduction potential, respectively. By changing the electron-donating segments, we successfully tailored the LUMO energy levels of the PDI-based polymers; the LUMO energy levels varied from 4.05 eV for PV-PDI to 3.61 eV for PF-PDI, which will help in the choice of appropriate donor materials for effective charge separation at the donor/acceptor interface and at the same time for higher V_{OC} .

For donor materials, the two polymers show similar electrochemical band gaps. However, the HOMO of PT1 decreases to 5.08 eV (P3HT: 4.91 eV). It is understood that the V_{OC} of PSCs is related to the energy difference between the LUMO of the acceptor (A) and the HOMO of the donor (D; [LUMO(A)-HOMO(D)]).^[4] The CV results indicate that we can successfully tune this difference by inducing either an upward shift in energy of the LUMO of PDI-based polymers or a downward shift in energy of the HOMO of polythiophene derivatives (Figure 2).

Prior to their use in all-PSC devices, it is necessary to confirm that the PDI-based polymers actually function as electron-transporting materials. To investigate the electron-transport properties of PX-PDIs in solid films, bottom-gate, top-contact field-effect transistors (FETs) were fabricated by spin-coating solutions of PX-PDIs in chloroform onto SiO_2/Si substrates modified with octadecyltrichlorosilane (OTS). All the transistors based on PX-PDIs exhibited typical n-type behavior, and distinct field effects were observed from the

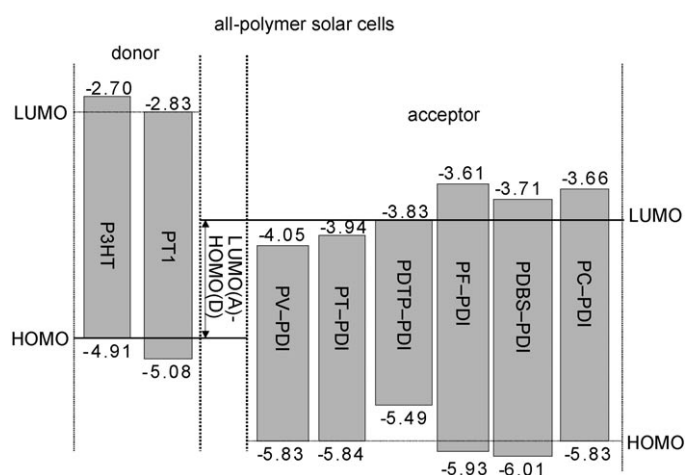


Figure 2. Energy level diagrams of various donor and acceptor polymers.

output characteristics (Figure S7). The electron mobilities without intensive optimization are estimated to be 10^{-4} – 10^{-3} $\text{cm}^2\text{V}^{-1}\text{s}^{-1}$ for all six PX-PDIs; these values are comparable to those of typical PDI-based polymers.^[8,9]

We investigated the photovoltaic properties of all possible combinations of the six PX-PDIs as electron acceptors and polythiophene derivatives as the electron donors. Firstly, we fabricated all-PSCs with a typical sandwich structure (glass/ITO/PEDOT:PSS/active layer/cathode; ITO = indium tin oxide, PEDOT:PSS = poly(styrenesulfonate)-doped poly(3,4-ethylenedioxythiophene)). The ratio of donor to acceptor, cathode material (Al, LiF/Al, and Ca/Al), solvents (CF, CB, and DCB), spin-coating speed, and postannealing temperature were optimized. In most cases, devices obtained by using CB as solvent, Ca/Al as cathode, and a donor/acceptor weight ratio of 2:1 without postannealing showed the best performance in each combination. The *I*-*V* curves of the optimized mixed BHJ devices for various combinations of the donor and acceptor polymers under illumination of AM 1.5 (100 mW cm^{-2}) is shown in Figure S8. The V_{OC} , I_{SC} , fill factor (FF), and PCE data of the various polymer combinations are summarized in Table 1.

The data show that the all-PSCs based on the PT1/PX-PDI blends had higher V_{OC} (0.58–0.76 V) than those of the devices based on the P3HT/PX-PDI blends (0.44–0.58 V). This result is in accordance with the values obtained by LUMO(A)-HOMO(D) (Figure 2). The relationship between V_{OC} and LUMO(A)-HOMO(D) is shown in Figure S9. Although a linear relationship was observed, the slopes of the linear fits for PT1/PX-PDI and P3HT/PX-PDI blends were 0.42 and 0.21 respectively, which is significantly less

than those observed for polymer/fullerene BHJs (typically close to one).^[11] This result might reflect the difference in the mixing morphology between polymer/fullerene and polymer/polymer BHJs, but the reason is not clear at this stage and further investigation is necessary. At the same time, the PT1/PX-PDI blends also showed higher short-circuit currents (I_{SC}) than their corresponding P3HT/PC-PDI blends, the reason for which is not as simple as that in the case of the V_{OC} . The I_{SC} of all-PSCs, similar to that of polymer/fullerene BHJ solar cells, is also influenced by the interpenetrating nanostructure formed by the two polymer blends.

To determine possible reasons for the higher I_{SC} of the PT1/PX-PDI blends than of the P3HT/PX-PDI blends, the morphology of the blend films was investigated by AFM and is shown in Figure 3. All blend films of P3HT/PX-PDI show a rough surface and coarse phase separa-

Table 1: Device characteristics of all-PSCs based on six acceptor- and two donor-polymers spin-coated from chlorobenzene.

Active layer		V_{OC} [V]	I_{SC} [mA cm^{-2}]	FF	PCE
Acceptor	Donor				
PV-PDI	P3HT	0.44	1.03	0.46	0.21%
	PT1	0.58	2.23	0.38	0.48%
PT-PDI	P3HT	0.50	0.70	0.58	0.20%
	PT1	0.62	3.24	0.49	0.97%
PDTP-PDI	P3HT	0.46	0.76	0.50	0.17%
	PT1	0.66	3.05	0.46	0.93%
PF-PDI	P3HT	0.52	0.39	0.53	0.11%
	PT1	0.76	1.77	0.43	0.58%
PDBS-PDI	P3HT	0.50	0.76	0.49	0.18%
	PT1	0.72	2.80	0.40	0.81%
PC-PDI	P3HT	0.58	0.91	0.55	0.29%
	PT1	0.74	3.31	0.47	1.15%

tion, which could be the reason for the lower I_{SC} of the photovoltaic devices compared to P3HT/PX-PDI. In contrast, all PT1/PX-PDI films, except PT1/PC-PDI, show a rather smooth surface and a more uniform mixing. This better miscibility of PT1/PX-PDI than of P3HT/PX-PDI explains, at least in part, the increased photocurrent. These results

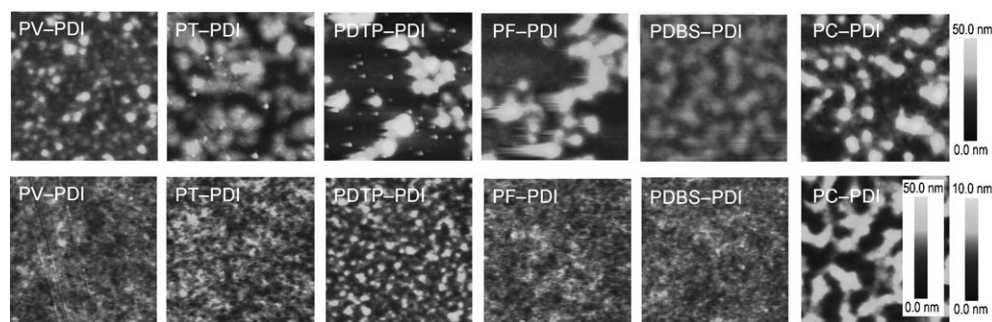


Figure 3. AFM height images of the surface of P3HT/PX-PDIs (top) and PT1/PX-PDIs (bottom) mixed bulk heterojunction layers spin-coated from chlorobenzene (dimensions: $2\text{ }\mu\text{m} \times 2\text{ }\mu\text{m}$).

suggest that PT1 is more compatible with PDI-based polymers (except PC-PDI) than P3HT in films cast from solutions in chlorobenzene; this may be related to the high crystallinity of regioregular P3HT.

It is important to note that even though the PT1/PC-PDI blend film shows a relatively rough morphology in the AFM height image, thus suggesting the coarse phase separation between the polymers, the solar cells of PT1:PC-PDI, among all the material combinations, gave the highest I_{SC} . This result implies that there is still room for improvement in terms of the charge separation interface in PT1/PC-PDI. Firstly, we tried to further optimize the film morphology by changing the spin-coating solvent. We tried common organic solvents such as xylene, toluene, CF, CB, and DCB, and found that xylene and toluene show an obvious improvement of the PCE to 1.32% and 1.85%, respectively. It has been shown previously that the use of suitable solvent mixtures can improve the morphology of the active layers,^[12] therefore we also tried various combinations of solvents for spin-coating. We found that toluene/CF 9:1 gives the best photovoltaic performance with a PCE of 2.23%, which exceeds the highest PCE previously reported for all-PSCs. The PSC obtained by using solvent mixtures showed good reproducibility, that is, an average PCE of 2.21% for five PSC devices. The I - V curves and detailed photovoltaic data obtained with the different solvents used for spin-coating are shown in Figure 4 and corresponding AFM images are shown in Figure 5.

The film surface morphology showed obvious improvement with the use of the solvent mixtures. Although it is quite difficult to measure them directly, the interpenetrating nanostructures were speculated to have been improved in the film spin-coated from the solvent mixtures.

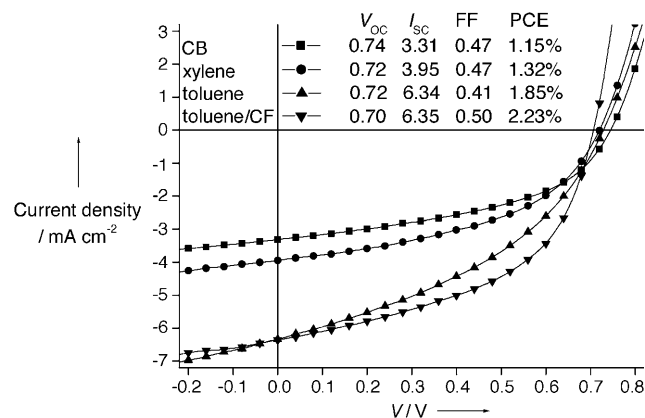


Figure 4. I - V curves and detailed photovoltaic data of all-PSCs based on PT1/PC-PDIs spin-coated from different solvents.

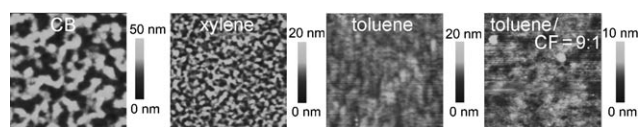


Figure 5. AFM height images of the surface of PT1/PC-PDIs spin-coated from different solvents (dimensions: $3 \mu\text{m} \times 3 \mu\text{m}$).

The difference between the LUMO levels of PT1 and PC-PDI is still relatively large (0.83 eV). This observation means that there still is room for lowering the LUMO level of PT1 or for raising the LUMO level of PDI-based n-type polymers, which would lead to a higher V_{OC} and at the same time a sufficient driving force for charge transfer would be maintained. Further fine-tuning of the energy levels of both p-type and n-type polymers by structural modification is currently in progress. Figure 6 shows the external quantum efficiency

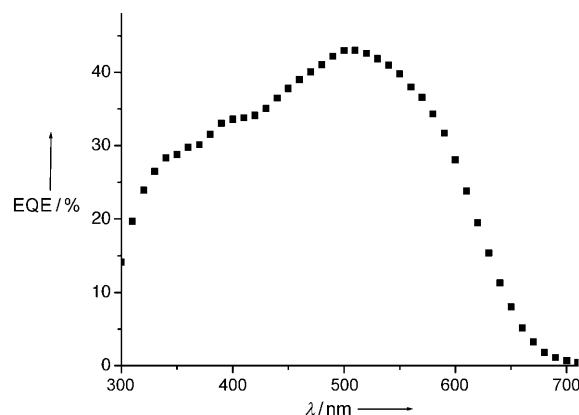


Figure 6. EQE spectrum of best all-PSC based on PT1/PC-PDI spin-coated from toluene/CF 9:1.

(EQE) plot of the optimized all-PSC device with the PT1/PC-PDI combination under illumination with monochromatic light. The EQE of the device covers most of the visible wavelength range from 300 to 700 nm with the highest value of 43% at 510 nm. The I_{SC} calculated from the EQE was approximately 10% lower than the measured I_{SC} , which may be attributed to the device degradation during measurements in air.

In summary, all-PSCs based on six perylene diimide containing polymers (PX-PDIs) as acceptor materials and two polythiophene derivatives (P3HT and PT1) as donor materials were investigated systematically. PT1/PX-PDIs showed obvious improvement in their device performance compared to the corresponding P3HT/PX-PDI combinations because of the better film morphology of PT1/PX-PDIs and the lower HOMO energy level of PT1 than that of P3HT. Owing to the use of solvent mixtures and the thus obtained phase-separation control, the highest PCE of all-PSCs based on PT1/PC-PDI reached 2.23%, which is one of the best PCE values of polymer/polymer blend photovoltaic devices reported to date. Considering the large improvement in all-PSCs with the use of PT1 as donor material instead of P3HT, further investigation on the combination of p-type and n-type polymers could lead to a higher PCE, comparable to that of polymer/fullerene BHJs.

Received: August 30, 2010

Revised: December 24, 2010

Published online: February 21, 2011

Keywords: nanotechnology · perylene diimide · polymers · photovoltaics · solar cells

- [1] a) C. J. Brabec, N. S. Sariciftci, J. C. Hummelen, *Adv. Funct. Mater.* **2001**, *11*, 15; b) F. C. Krebs, *Sol. Energy Mater. Sol. Cells* **2009**, *93*, 394; c) F. C. Krebs, M. Jorgensen, K. Norrman, O. Hagemann, J. Alstrup, T. D. Nielsen, J. Fyenbo, K. Larsen, J. Kristensen, *Sol. Energy Mater. Sol. Cells* **2009**, *93*, 422; d) F. C. Krebs, S. A. Gevorgyan, J. Alstrup, *J. Mater. Chem.* **2009**, *19*, 5442; e) F. C. Krebs, T. D. Nielsen, J. Fyenbo, M. Wadström, M. S. Pedersen, *Energy Environ. Sci.* **2010**, *3*, 512; f) F. C. Krebs, T. Tromholt, M. Jørgensen, *Nanoscale* **2010**, *2*, 873; g) J. Y. Jung, Z. Y. Guo, S. W. Jee, H. D. Um, K. T. Park, J. H. Lee, *Opt. Express* **2010**, *18*, A286; h) M. Helgesen, R. Søndergaard, F. C. Krebs, *J. Mater. Chem.* **2010**, *20*, 36.
- [2] a) J. Peet, J. Y. Kim, N. E. Coates, W. L. Ma, D. Moses, A. J. Heeger, G. C. Bazan, *Nat. Mater.* **2007**, *6*, 497; b) J. H. Hou, H. Y. Chen, S. Q. Zhang, G. Li, Y. Yang, *J. Am. Chem. Soc.* **2008**, *130*, 16144; c) Y. Y. Liang, D. Q. Feng, Y. Wu, S.-T. Tsai, G. Li, C. Ray, L. P. Yu, *J. Am. Chem. Soc.* **2009**, *131*, 7792; d) S. H. Park, A. Roy, S. Beaupré, S. Cho, N. Coates, J. S. Moon, D. Moses, M. Leclerc, K. Lee, A. J. Heeger, *Nat. Photonics* **2009**, *3*, 297; e) H.-Y. Chen, J. H. Hou, S. Q. Zhang, Y. Y. Liang, G. W. Yang, Y. Yang, L. P. Yu, Y. Wu, G. Li, *Nat. Photonics* **2009**, *3*, 649.
- [3] M. M. Wienk, J. M. Kroon, W. J. H. Verhees, J. Knol, J. C. Hummelen, P. A. van Hal, R. A. J. Janssen, *Angew. Chem.* **2003**, *115*, 3493; *Angew. Chem. Int. Ed.* **2003**, *42*, 3371.
- [4] a) C. J. Brabec, A. Cravino, D. Meissner, N. S. Sariciftci, T. Fromherz, M. T. Rispens, L. Sanchez, J. C. Hummelen, *Adv. Funct. Mater.* **2001**, *11*, 374; b) B. C. Thompson, J. M. J. Fréchet, *Angew. Chem.* **2008**, *120*, 62; *Angew. Chem. Int. Ed.* **2008**, *47*, 58.
- [5] a) M. Lenes, G. A. H. Wetzelaer, F. B. Kooistra, S. C. Veenstra, J. C. Hummelen, P. W. M. Blom, *Adv. Mater.* **2008**, *20*, 2116; b) R. B. Ross, C. M. Cardona, D. M. Guldi, S. G. Sankaranarayanan, M. O. Reese, N. Kopidakis, J. Peet, B. Walker, G. C. Bazan, E. V. Keuren, B. C. Holloway, M. Grees, *Nat. Mater.* **2009**, *8*, 208; c) Y. J. He, H.-Y. Chen, J. H. Hou, Y. F. Li, *J. Am. Chem. Soc.* **2010**, *132*, 1377.
- [6] C. R. McNeill, N. C. Greenham, *Adv. Mater.* **2009**, *21*, 3840.
- [7] a) M. Granström, K. Petritsch, A. C. Arias, A. Lux, M. R. Andersson, R. H. Friend, *Nature* **1998**, *395*, 257; b) T. W. Holcombe, C. H. Woo, D. F. J. Kavulak, B. C. Thompson, J. M. J. Fréchet, *J. Am. Chem. Soc.* **2009**, *131*, 14160; c) X. M. He, F. Gao, G. L. Tu, D. Hasko, S. Hüttner, U. Steiner, N. C. Greenham, R. H. Friend, W. T. S. Huck, *Nano Lett.* **2010**, *10*, 1302.
- [8] X. W. Zhan, Z. A. Tan, B. Domercq, Z. S. An, X. Zhang, S. Barlow, Y. F. Li, D. B. Zhu, B. Kippelen, S. R. Marder, *J. Am. Chem. Soc.* **2007**, *129*, 7246.
- [9] a) Z. A. Tan, E. J. Zhou, X. W. Zhan, X. Wang, Y. F. Li, S. Barlow, S. R. Marder, *Appl. Phys. Lett.* **2008**, *93*, 073309; b) L. J. Huo, Y. Zhou, Y. F. Li, *Macromol. Rapid Commun.* **2008**, *29*, 1444; c) X. W. Zhan, Z. A. Tan, E. J. Zhou, Y. F. Li, R. Misra, A. Grant, B. Domercq, X. H. Zhang, Z. S. An, X. Zhang, S. Barlow, B. Kippelen, S. R. Marder, *J. Mater. Chem.* **2009**, *19*, 5794; d) J. A. Mikroyannidis, M. M. Stylianakis, G. D. Sharma, P. Balraju, M. S. Roy, *J. Phys. Chem. C* **2009**, *113*, 7904; e) E. J. Zhou, K. Tajima, C. H. Yang, K. Hashimoto, *J. Mater. Chem.* **2010**, *20*, 2362.
- [10] Y. F. Li, Y. P. Zou, *Adv. Mater.* **2008**, *20*, 2952.
- [11] M. C. Scharber, D. Mühlbacher, M. Koppe, P. Denk, C. Waldauf, A. J. Heeger, C. J. Brabec, *Adv. Mater.* **2006**, *18*, 789.
- [12] a) M. M. Wienk, M. Turbiez, J. Gilot, R. A. J. Janssen, *Adv. Mater.* **2008**, *20*, 2556; b) D. Kitazawa, N. Watamabe, S. Yamamoto, J. Tsukamoto, *Appl. Phys. Lett.* **2009**, *95*, 053701.